JACS
JOURNAL OF THE AMERICAN CHEMICAL SOCIETY

Subscriber access provided by American Chemical Society

Article

Metal-Core–Organic Shell Dendrimers as Unimolecular Micelles

K. R. Gopidas, James K. Whitesell, and Marye Anne Fox

J. Am. Chem. Soc., **2003**, 125 (46), 14168-14180• DOI: 10.1021/ja036626h • Publication Date (Web): 28 October 2003

Downloaded from http://pubs.acs.org on March 30, 2009

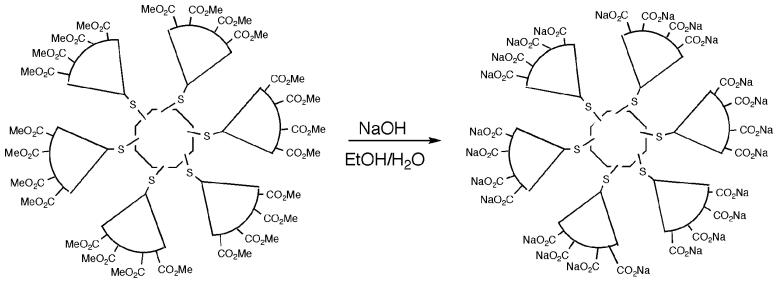

More About This Article

Additional resources and features associated with this article are available within the HTML version:

- Supporting Information
- Links to the 6 articles that cite this article, as of the time of this article download
- Access to high resolution figures
- Links to articles and content related to this article
- Copyright permission to reproduce figures and/or text from this article

View the Full Text HTML

ACS Publications
High quality. High impact.

Journal of the American Chemical Society is published by the American Chemical Society. 1155 Sixteenth Street N.W., Washington, DC 20036

J|A|C|S
ARTICLES
Published on Web 10/28/2003

Metal-Core−Organic Shell Dendrimers as Unimolecular Micelles

K. R. Gopidas,† James K. Whitesell,* and Marye Anne Fox*

Contribution from the Department of Chemistry, North Carolina State University, Campus Box 8204, Raleigh, North Carolina 27695

Received June 11, 2003; E-mail: mafox@ncsu.edu

Abstract: The synthesis and characterization of nanoparticle-cored dendrimers (NCDs), consisting of a metal core capped by arylpolyethers terminated with ester or carboxylate groups, are reported. These NCDs, comprising nanometer-sized gold clusters at the core and organic dendrons radially connected to the gold core by gold−sulfur bonds, were analyzed by TEM, TGA, UV, IR, and NMR spectroscopies. The density of the branching units connected to the core decreased from 1.90/nm^2 for a first-generation NCD (Au−G1(CO_2Me)) to 0.80/nm^2 for a fourth-generation NCD (Au−G4(CO_2Me)). Although the ester-terminated NCDs were stable and resisted aggregation, they were easily hydrolyzed to the corresponding water-soluble sodium salts. Aqueous solutions of (Au−G*n*(CO_2Na)) exhibited micellar properties. Since these NCDs possess a relatively unpassivated metal core and an organic aryl ether shell with micellar and dendritic properties, they are expected to have important potential applications in catalysis.

Introduction

The correlation between structure and function of designed molecules is one of the most fundamental issues of chemistry. The vast array of possible structural variations in dendritic architectures[1] make functional dendrimers a particularly important group with which to probe such relationships. Dendrimers are three-dimensional macromolecules possessing three distinguishing structural components, namely (a) an interior core, (b) bridging layers often called "generations" (G) composed of repeating units radially attached to the core, and (c) a layer of terminal groups attached to the outermost branching unit. These components determine the overall size, shape, and physicochemical properties of the dendrimer. A variety of structural modifications are possible for each of these units, resulting in a large array of dendritic molecules with potential applications in molecular recognition, catalysis, magnetic resonance imaging, and light harvesting.[2] They are likely to find practical use as nanodevices, chemical and biochemical sensors, pharmaceuticals, drug-delivery agents, self-organizing assemblies, and membrane- and micelle mimics.

For these intriguing possible deployments, the incorporation of metals into the dendritic framework is of particular interest.[3] Three general categories of metal-ion-containing dendrimers have been described in the literature. The first category consists of dendrimers having metal ions as an integral part of their structure.[4] Examples include dendrimers having an organometallic core and those that use metal-ion ligation to assemble the dendrimeric branches. The second category consists of dendrimers having peripheral groups that can bind metal ions.[5] Metal-ion binding in these cases can be electrostatic (as in carboxylate-terminated dendrimers) or coordinative (as in terpyridine- or phosphine-terminated dendrimers). The third category

† Permanent address: Photosciences and Photonics Division, Regional Research Laboratory (CSIR), Trivandrum - 695 019, India.

(1) (a) Tomalia, D. A.; Naylor, A. M.; Goddard, W. A. III. *Angew. Chem., Int. Ed. Engl.* **1990**, *29*, 138. (b) Vögtle, F., Schalley, C. A., Eds. *Dendrimers IV: Metal Coordination, Self-Assembly, Catalysis*; Topics in Current Chemistry, No. 217; Springer-Verlag: Berlin, 2001. (c) Vögtle, F., Ed. *Dendrimers III: Design, Dimension, Function*; Topics in Current Chemistry, No. 212; Springer-Verlag: Berlin, 2001. (d) Fréchet. J. M. J., Tomalia, D. A., Eds. *Dendrimers and Other Dendritic Polymers*; John-Wiley & Sons: Chichester, 2001. (e) Vögtle, F., Ed. *Dendrimers II: Architecture, Nanostructure and Supramolecular Chemistry*; Topics in Current Chemistry, No. 210; Springer-Verlag: Berlin, 2000. (f) Vögtle, F., Ed. *Dendrimers*; Topics in Current Chemistry, No. 197; Springer-Verlag: Berlin, 1998. (g) Newkome, G. R., Moorefield, C. N., Vögtle, F. *Dendritic Molecules: Concepts, Synthesis, Applications*; Wiley-VCH: Weinheim, 2001.

(2) (a) van Heerbeek, R.; Kamer, P. C. J.; van Leeuwen, P. W. N. M.; Reek, J. N. H. *Chem. Rev.* **2002**, *102*, 3717. (b) Bezouska, K. *Rev. Mol. Biotechnol.* **2002**, *90*, 269. (c) Reek, J. N. H.; de Groot, D.; Oosterom, G. E.; Kamer, P. C. J.; van Leeuwen, P. W. N. M. *Rev. Mol. Biotechnol.* **2002**, *90*, 159. (d) Twyman, L. J.; King, A. S. H.; Martin, I. K. *Chem. Soc. Rev.* **2002**, *31*, 69. (e) Astruc, D.; Chardac, F. *Chem. Rev.* **2001**, *101*, 2991. (f) Tully, D. C.; Fréchet, J. M. J. *Chem. Com.* **2001**, 1229. (g) Oosterom, G. E.; Reek, J. N. H.; Kamer, P. C. J.; van Leeuwen, P. W. N. M. *Angew. Chem., Int. Ed.* **2001**, *40*, 1828. (h) Shamsi, S. A.; Palmer, C. P.; Warner, I. M. *Anal. Chem.* **2001**, *73*, 140. (i) Duncan, R. *Polym. Mater. Sci. Eng.* **2001**, *84*, 214. (j) Dykes, G. M. *J. Chem. Technol. Biotechnol.* **2001**, *76*, 903.(k) Vögtle, F.; Gestermann, S.; Hesse, R.; Schwierz, H.; Windisch, B. *Prog. Polym. Sci.* **2000**, *25*, 987. (l) Bosman, A. W.; Janssen, H. M.; Meijer, E. W. *Chem. Rev.* **1999**, *99*, 1665.

(3) (a) Fischer, M.; Vögtle, F. *Angew. Chem., Int. Ed.* **1999**, *38*, 884. (b) Frey, H.; Lach, C.; Lorenz, K. *Adv. Mater.* **1998**, *10*, 279. (c) Balzani, V.; Campagna, S.; Denti, G.; Juris, A.; Serroni, S.; Venturi, M. *Acc. Chem. Res.* **1998**, *31*, 26. (d) Zeng, F.; Zimmerman, S. C. *Chem. Rev.* **1997**, *97*, 1681.

(4) (a) Jian, D. L.; Aida, T. *J. Chem. Soc., Chem. Commun.* **1996**, 1523. (b) Enomoto, M.; Aida, T. *J. Am. Chem. Soc.* **1999**, *121*, 874. (c) Dandliker, P. J.; Diederich, F.; Gross, M.; Knobler, M.; Louati, A.; Sanford, E. M. *Angew. Chem., Int. Ed. Engl.* **1994**, *33*, 1739. (d) Bhyrappa, P.; Young, J. K.; Moore, J. S.; Suslick, K. S. *J. Am. Chem. Soc.* **1996**, *118*, 5708. (e) Pollak, K. W.; Leon, J. W., Fréchet, J. M. J.; Maskus, M.; Abruna, H. D. *Chem. Mater.* **1998**, *10*, 30. (f) Newkome, G. R.; Guther, R.; Moorefield, C. N.; Cardullo, F.; Echegoyen, L.; Perezcordero, E.; Luftmann, H. *Angew. Chem., Int. Ed. Engl.* **1995**, *34*, 2023. (g) Chow, H. F.; Chan, I. Y. K.; Chan, D. T. W.; Kwok, R. W. M. *Chem. Eur. J.* **1996**, *2*, 1085. (h) Gorman, C. B.; Smith, J. C.; Hagar, M. W.; Parkhurst, B. L.; Sierzputowska-Gracz, H.; Haney, C. A. *J. Am. Chem. Soc.* **1999**, *121*, 9958.

10.1021/ja036626h CCC: $25.00 **© 2003 American Chemical Society**

Scheme 1. Preparation of Ester-Terminated Au−NCDs

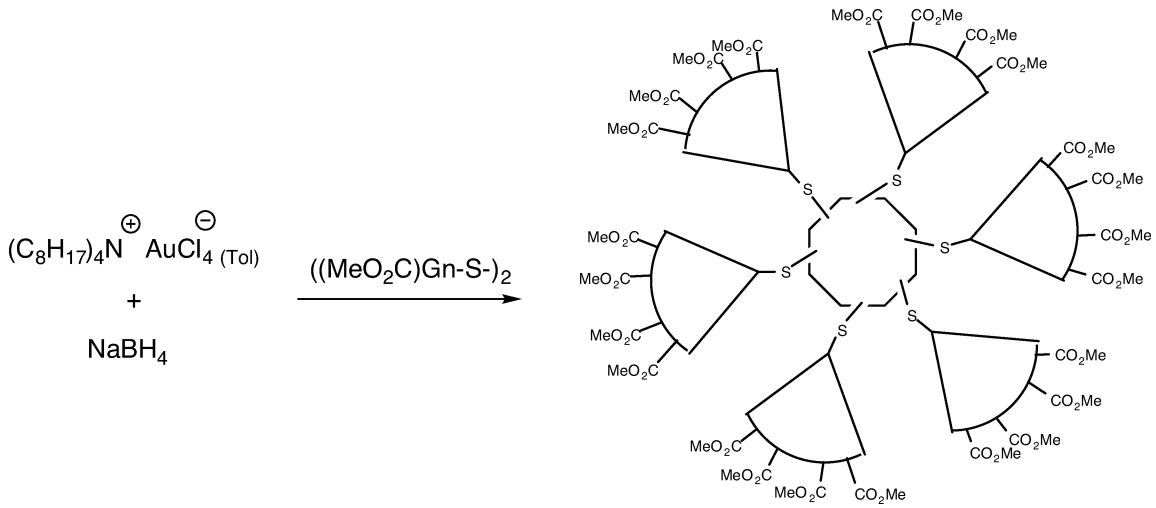

consists of dendrimers that encapsulate metal ions.[6] These dendrimers generally contain functional groups that can coordinate metal ions in their interior.

It has been demonstrated recently[7] that metal ions encapsulated within a dendrimer can be reduced chemically, producing composite dendrimers containing very small, encapsulated metal clusters within the organic dendrimeric structure. The resulting metal clusters are protected from agglomeration by the encasing dendrimer. If a substantial fraction of their surface is nonpassivated, these zerovalent metal clusters would be active in catalytic reactions, and several applications of such dendrimer-encapsulated nanoparticles in catalysis have been well demonstrated.[8]

In a recent contribution,[9] we reported the synthesis and characterization of a fourth group of metal-containing dendrimers, namely, nanoparticle-cored dendrimers (NCD). These dendrimers have gold nanoparticles at the core to which are attached dendrimers generated by the self-assembled binding of disulfide-containing dendrons on the nanoparticle surface. Our strategy makes use of the Brust reaction,[10] which was originally designed for the preparation of monolayer-protected clusters (MPC) of noble metals, as the final step in the dendrimer synthesis. In the original Brust synthesis, dodecanethiolate-protected gold clusters of 1−3 nm core diameter were prepared by reducing a solution of tetrachloroaurate in the presence of dodecanethiol. Subsequent reports[11] have shown that a wide range of alkanethiolate chain lengths (C_3−C_{24}), ω-functionalized alkanethiolates, arenethiolates, and dialkylsulfides can be employed in the same protocol.

We have demonstrated that reduction of $HAuCl_4$ phase-transferred into toluene using tetraoctylammonium bromide (TOAB) in the presence of polyaryl ether disulfide dendrons resulted in the formation of gold nanoparticle-cored dendrimers (Au-NCD), Scheme 1. Au-NCDs may be formed either by the direct self-assembly of disulfide dendrons or by the self-assembly of thiol-functionalized dendrons formed from the corresponding disulfides under the reducing conditions employed in the NCD synthesis. The latter suggestion is based on recent work by Tomalia et al., who showed that disulfide-cored dendrons cleave to produce the corresponding thiols under reducing conditions.[12] The Au-NCDs thus produced were analyzed by transmission electron microscopy (TEM), thermogravimetric analysis (TGA), ultraviolet absorption (UV) spec-

(5) (a) Newkome, G. R.; Cardullo, F.; Constable, E. C.; Moorefield, C. N.; Thompson, A. M. W. C. *J. Chem. Soc., Chem. Commun*. **1993**, 925. (b) Alonso, B.; Cuadrado, I.; Moran, M.; Losada, J. *J. Chem. Soc., Chem. Commun*. **1994**, 2575. (c) Takada, K.; Diaz, D. J.; Abruna, H. D.; Cuadrado, I.; Casado, C.; Alonso, B.; Moran, M.; Losada, J. *J. Am. Chem. Soc*. **1997**, *119*, 10763. (d) Kriesel, J. W.; König, S.; Freitas, M. A.; Marshall, A. G.; Leary, J. A.; Tilley, T. D. *J. Am. Chem. Soc*. **1998**, *120*, 12207. (e) Zhao, M.; Sun, L.; Crooks, R. M. *J. Am. Chem. Soc*. **1998**, *120*, 4877. (f) Ottaviani, M. F.; Ghatlia, N. D.; Bossmann, S. H.; Barton, J. K.; Durr, H.; Turro, N. J. *J. Am. Chem. Soc*. **1992**, *114*, 8946. (g) Ottaviani, M. F.; Bossmann, S.; Turro, N. J.; Tomalia, D. A. *J. Am. Chem. Soc*. **1994**, *116*, 661.

(6) (a) Chechik, V.; Zhao, M.; Crooks, R. M. *J. Am. Chem. Soc*. **1999**, *121*, 4910. (b) Zhou, L.; Russel, D. H.; Zhao, M.; Crooks, R. M. *Macromolecules* **2001**, *34*, 3567. (c) Ottaviani, M. F.; Turro, N. J.; Jockusch, S.; Tomalia, D. A. *J. Phys. Chem*. **1996**, *100*, 13675. (d) Garcia, M. E.; Baker, L. A.; Crooks, R. M. *Anal. Chem*. **1999**, *71*, 256.

(7) (a) R. M. Crooks, Zhao, M.; Sun, L.; Chechik, V.; Yeung, L. K. *Acc. Chem. Res*. **2001**, *34*, 181. (b) Zhao, M.; Crooks, R. M. *Chem. Mater*. **1999**, *11*, 3379. (c) Zhao, M.; Crooks, R. M. *Adv. Mater*. **1999**, *11*, 217. (d) Balogh, L.; Tomalia, D. A. *J. Am. Chem. Soc*. **1998**, *120*, 7355.

(8) (a) Chechik, V.; Crooks, R. M. *J. Am. Chem. Soc*. **2000**, *122*, 1243. (b) Yeung, L. K.; Lee, C. T., Jr.; Johnston, K. P.; Crooks, R. M. *Chem. Commun*. **2001**, 2290. (c) Yeung, L. K.; Crooks, R. M. *Nano Lett*. **2001**, *1*, 14. (c) Rahim, E. H.; Kamounah, F. S.; Frederiksen, J.; Christensen, J. B. *Nano Lett*. **2001**, *1*, 499. (d) Niu, Y.; Yeung, L. K.; Crooks, R. M. *J. Am. Chem. Soc*. **2001**, *123*, 6840. (e) Zhao, M.; Crooks, R. M. *Angew. Chem., Int. Ed*. **1999**, *38*, 364.

(9) Gopidas, K. R.; Whitesell, J. K.; Fox, M. A. *J. Am. Chem. Soc*. **2003**, *125*, 6491.

(10) Brust, M.; Walker, M.; Bethel, D.; Schiffrin, D. J.; Whyman, R. *J. Chem. Soc., Chem. Commun*. **1994**, 801.

(11) (a) Hostetler, M. J.; Green, S. J.; Stokes, J. J.; Murray, R. W. *J. Am. Chem. Soc*. **1996**, *118*, 4212. (b) Green, S. J.; Stokes, J. J.; Hostetler, M. J.; Pietron, J.; Murray, R. W. *J. Phys. Chem. B* **1997**, *101*, 2663. (c) Ingram, R. S.; Hostetler, M. J.; Murray, R. W. *J. Am. Chem. Soc*. **1997**, *119*, 9175. (d) Wuelfing, W. P.; Gross, S. M.; Miles, D. T.; Murray, R. W. *J. Am. Chem. Soc*. **1998**, *120*, 12696. (e) Hostetler, M. J.; Zhong, C.-J.; Yen, B. K. H.; Anderegg, J.; Gross, S. M.; Evans, N. D.; Porter, M.; Murray, R. W. *J. Am. Chem. Soc*. **1998**, *120*, 9396. (f) Templeton, A. C.; Hostetler, M. J.; Kraft, C. Y.; Murray, R. W. *J. Am. Chem. Soc*. **1998**, *120*, 1906. (g) Templeton, A. C.; Hostetler, M. J.; Warmoth, E. K.; Chen, S.; Hartshorn, C. M.; Krishnamurthy, V. M.; Forbes, M. D. E.; Murray, R. W. *J. Am. Chem. Soc*. **1998**, *120*, 4845. (h) Ingram, R. S.; Murray, R. W. *Langmuir* **1998**, *14*, 4115. (i) Green, S. J.; Pietron, J. J.; Stokes, J. J.; Hostetler, M. J.; Vu, H.; Wuelfing, W. P.; Murray, R. W. *Langmuir* **1998**, *14*, 5612. (j) Johnson, S. R.; Evans, S. D.; Brydson, R. *Langmuir* **1998**, *14*, 6639. (k) Chen, S.; Murray, R. W. *Langmuir* **1999**, *15*, 682. (l) Porter, L. A.; Ji, D.; Westcott, S. L.; Graupe, M.; Czernuszewicz, R. S.; Halas, N. J.; Lee, T. R. *Langmuir* **1998**, *14*, 7378. (m) Cliffel, D. E.; Zamborini, F. P.; Gross, S. M.; Murray, R. W. *Langmuir* **2000**, *16*, 9699. (n) Templeton, A. C.; Wuelfing, W. P.; Murray, R. W. *Acc. Chem. Res*. **2000**, *33*, 27. (o) Shon, Y.-S.; Gross, S. M.; Dawson, B.; Porter, M.; Murray, R. W. *Langmuir* **2000**, *16*, 6555. (p) Hu, J.; Zhang, J.; Liu, F.; Kittredge, K.; Whitesell, J. K.; Fox, M. A. *J. Am. Chem. Soc*. **2001**, *123*, 1464. (q) Zamborini, F. P.; Gross, S. M.; Murray, R. W. *Langmuir* **2001**, *17*, 481. (r) Fang, H.; Du, C.; Qu, S.; Li, Y.; Song, Y.; Li, H.; Liu, H.; Zhu. D. *Chem. Phys. Lett*. **2002**, *364*, 290. (s) Yang, W.; Chen, M.; Knoll, W.; Deng, H. *Langmuir* **2002**, *18*, 4124.

(12) Tomalia, D. A.; Huang, B.; Swanson, D. R.; Brothers, H. M., II; Klimash, J. W. *Tetrahedron*, **2003**, *59*, 3799.

Scheme 2. Basic Hydrolysis of Ester-Terminated NCDs to Produce Unimolecular Micelles

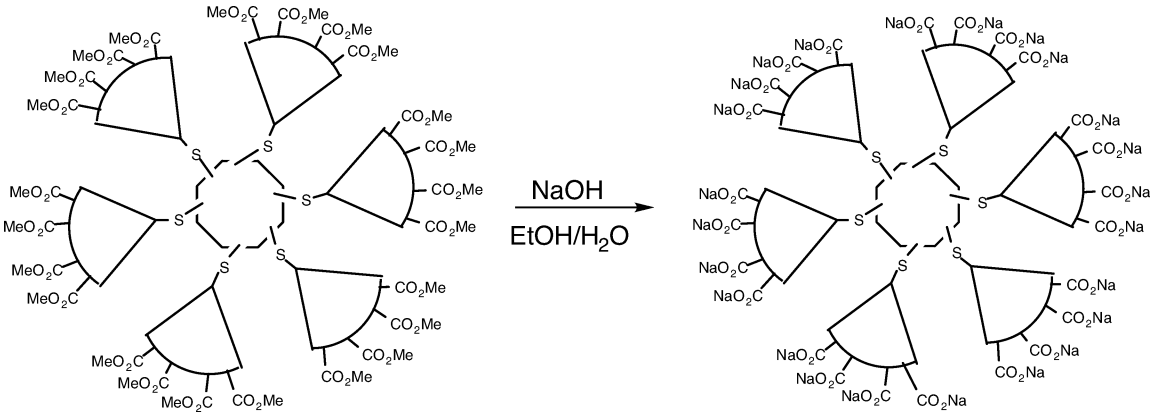

troscopy, infrared (IR) spectroscopy, and nuclear magnetic resonance (NMR) spectroscopy. We compare the structures of these Au-NCDs with classical dendrimers and MPCs and provide preliminary evidence that the NCDs may have important potential applications in catalysis.[9]

Peng and co-workers recently reported the synthesis and characterization of semiconductor (CdSe/CdS)-cored dendrimers and dendrimer boxes[13] analogous to our NCDs. The semiconductor core in these materials could be dissolved in concentrated HCl to give empty dendritic boxes, which are expected to have interesting host−guest properties.

The NCDs reported here are structurally similar to unimolecular micelles, as was first recognized by Newkome, as early as 1985.[14] Micelles are dynamic aggregates of amphilic molecules that have a nonpolar, hydrocarbon-like interior and a polar or ionic exterior when dispersed in solution.[15] Reverse micelles, on the other hand, have a polar hydrophilic interior and a hydrocarbon-like exterior. Micellization of the amphiphile occurs above a concentration known as the critical micelle concentration (cmc).

Organic dendrimers with amphiphilic moieties have been shown to exhibit micelle-like properties in solution.[16] In contrast to conventional micelles, which are aggregates that are constantly forming and reverting in an equilibrium process, the groups bound to the core in dendritic micelles are linked covalently, and therefore a fixed structure is maintained at all concentration ranges. Both normal and reverse dendritic unimolecular micelles have been reported to act as catalysts and as drug-delivery agents.[2,16]

This contribution describes the synthesis and characterization of organic−inorganic composite nanoparticle-cored dendrimers that can also function as unimolecular micelles with anionic surface charge. This was achieved when the terminal ester groups were hydrolyzed to the corresponding sodium carboxylate salts, Scheme 2.

As sodium salts, the NCDs were soluble in water and exhibited micellar properties. Spectral characterization of NCDs of generation 1−4 for the ester-terminated NCDs (Au−G*n*(CO_2Me)) and the corresponding sodium salts (Au−G*n*(CO_2Na)) are presented here.

Results and Discussion

Fréchet-type polyaryl ether dendrons with ester groups on the periphery (Chart 1), required for the synthesis of gold NCDs, were prepared by reported procedures.[16m]

The known dendritic bromides were converted to the corresponding thiols or disulfides by a procedure developed by Hu and Fox,[17] using hexamethyldisilathiane and tetrabutylammonium fluoride, Scheme 3.

To force the reaction to completion, excess hexamethyldisilathiane and tetrabutylammonium fluoride and extended reaction times were used. This procedure resulted in the production of a mixture of thiol and disulfide. In the lower-generation dendrons (G1 and G2), both thiols and disulfides were isolated and characterized. For the G3 and G4 dendrons, only disulfides were isolated from the reaction mixtures. The thiol and disulfide dendrons were purified by column chromatography and characterized by spectroscopic techniques. The purified disulfide dendrons (Chart 1) were used in the preparation of the gold NCDs described below.

Gold NCDs were prepared by the Brust reaction.[10] $HAuCl_4$ was phase-transferred into toluene using TOAB. The disulfide dendron, ((MeO$_2$C)G1-S-)$_2$−((MeO$_2$C)G4-S-)$_2$), dissolved in a small amount of methylene chloride, was then added. The mixture was cooled in ice (0−2 °C), and an excess of $NaBH_4$

(13) Guo, W.; Li, J. J.; Peng, X. *J. Am. Chem. Soc*. **2003**, *125*, 3901.
(14) Newkome, G. R.; Yao, Z.-Q.; Baker, G. R.; Gupta, V. K. *J. Org. Chem*. **1985**, *50*, 2003.
(15) (a) Tanford, C. *The Hydrophobic Effect: Formation of Micelles and Biological Membranes*; Wiley: New York, 1980. (b) Fendler, J. H.; Fendler, E. J. *Catalysis in Micellar and Macromolecular Systems*; Academic: New York, 1975. (c) Mukerjee, P.; Mysels, K. J. *Critical Micelle Concentrations of Aqueous Surfactant Systems*; Government Printing Office: Washington DC, 1971.
(16) (a) Fu, K.; Kitaygorodskiy, A.; Sun, Y.-P. *Chem. Mater*. **2000**, *12*, 2073. (b) Liu, M.; Kono, K.; Fréchet, J. M. J. *J. Controlled Release* **2000**, *65*, 121. (c) Liu, M.; Fréchet, J. M. J. *Polym. Bull*. **1999**, *43*, 379. (d) Piotti, M. E.; Rivera, F., Jr.; Bond, R.; Hawker, C. J.; Fréchet, J. M. J. *J. Am. Chem. Soc*. **1999**, *121*, 9471. (e) Stevelmans, S.; van Hest, J. C. M.; Jansen, J. F. G. A.; van Boxtel, D. A. F. J.; de Brabander van den Berg, E. M. M.; Meijer, E. W. *J. Am. Chem. Soc*. **1996**, *118*, 7398. (f) Schmitzer, A.; Perez, E.; Rico-Latters, I.; Lattes, A.; Rosca, S. *Langmuir* **1999**, *15*, 4397. (g) Liu, M.; Fréchet, J. M. J. *Polym. Mater. Sci. Eng*. **1999**, *80*, 167. (h) McElhanon, J. R.; McGrath, D. V. *Polym. Mater. Sci. Eng*. **1997**, *77*, 153. (i) Baars, M. W. P. L.; Meijer, E. W. *Polym. Mater. Sci. Eng*. **1997**, *77*, 149. (j) Pollak, K. W.; Fréchet, J. M. J. *Polym. Mater. Sci. Eng*. **1996**, *75*, 273. (k) Mattei, S.; Seiler, P.; Diederich, F.; *Helv. Chim. Acta* **1995**, *78*, 1904. (l) Kuzdzal, S. A.; Monnig, C. A.; Newkome, G. R.; Moorefield, C. N. *J. Chem. Soc., Chem. Commun*. **1994**, 2139. (m) Hawker, C. J.; Wooley, K. L.; Fréchet, J. M. J. *J. Chem. Soc., Perkin Trans. 1* **1993**, 1287. (n) Newkome, G. R.; Young, J. K.; Baker, G. R.; Potter, R. L.; Audoly, L.; Cooper, D.; Weis, C. D.; Morris, K.; Johnson, C. S., Jr. *Macromolecules* **1993**, *26*, 2394. (o) Lochmann, L.; Wooley, K. L.; Ivanova, P. T.; Fréchet, J. M. J. *J. Am. Chem. Soc*. **1993**, *115*, 7043. (p) Newkome, G. R.; Moorefield, C. N.; Baker, G. R.; Johnson, A. L.; Behera, R. K. *Angew. Chem., Int. Ed. Engl*. **1991**, *30*, 1176. (q) Newkome, G. R.; Moorefield, C. N.; Baker, G. R.; Saunders: M. J.; Grossman, S. H. *Angew. Chem., Int. Ed. Engl*. **1991**, *30*, 1178. (r) Tomalia, D. A.; Berry, V.; Hall, M.; Hedstrand, D. M. *Macromolecules* **1987**, *20*, 1167.
(17) Hu, J.; Fox, M. A. *J. Org. Chem*. **1999**, *64*, 4959.

Chart 1. Structures of Disulfide Dendrons Used in the Synthesis of NCDs

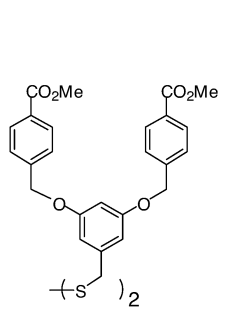

((MeO$_2$C)G1-S-)$_2$

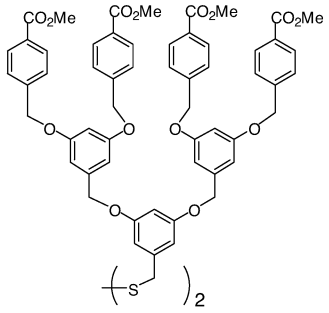

((MeO$_2$C)G2-S-)$_2$

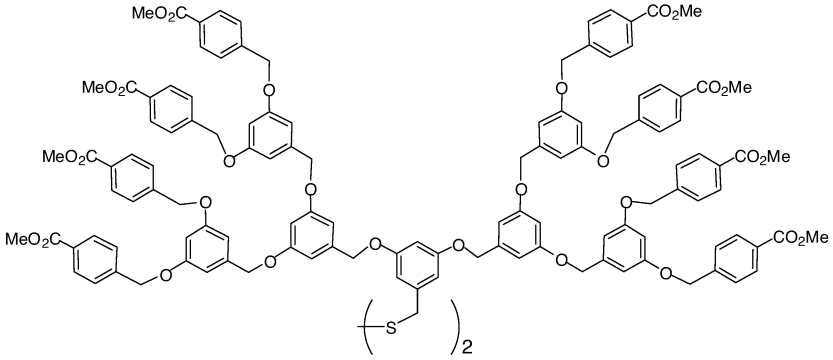

((MeO$_2$C)G3-S-)$_2$

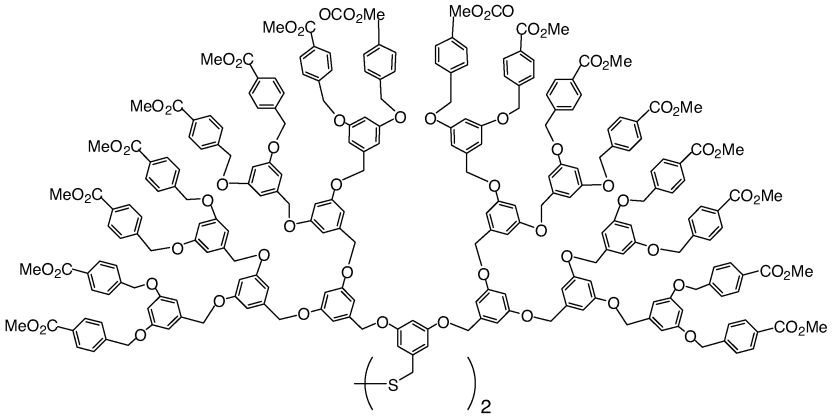

((MeO$_2$C)G4-S-)$_2$

was added. The resulting black solution was stirred for 2 days at room temperature. No precipitation or formation of insoluble materials was observed during any of these preparations. The toluene layer was then separated, and the NCDs were isolated using a standard protocol.[10] IR and NMR spectra of the NCDs show that the ester groups were unaffected by the reduction procedure.

The NCDs thus prepared were black powders, soluble in methylene chloride, chloroform, toluene, and THF. Dilute solutions of Au−G1(CO_2Me) and Au−G2(CO_2Me) were brown in color (cola-colored), whereas those of Au−G3(CO_2Me) and Au−G4(CO_2Me) appeared pink. These compounds are very stable in solution and in solvent-free forms. All of the NCDs were insoluble in methanol, ethanol, and diethyl ether. All of the NCDs trapped, as formed, some amount of TOAB (used as the phase transfer agent in the Brust reaction). The salt could not be removed completely even by repeated extraction with ethanol.

As a control experiment, the Brust reaction was carried out using the precursor bromo dendrons (MeO_2C)G1-Br−(MeO_2C)-G4-Br, instead of the disulfide dendrons. In all cases the reactions yielded black particles, the solubility of which depended on the generation of the dendrons. Particles obtained form the reaction of (MeO_2C)G1-Br were insoluble in CH_2Cl_2. Particles from the (MeO_2C)G2-Br reaction dissolved in CH_2Cl_2, but complete precipitation of the bare metal cluster occurred within a few minutes. Particles from the (MeO_2C)G3-Br and (MeO_2C)G4-Br reactions dissolved in CH_2Cl_2, and complete precipitation of the metal in these cases took 5−8 h. We have not analyzed these systems in any further detail, but the

Scheme 3. Sulfidation of Brominated Dendrons

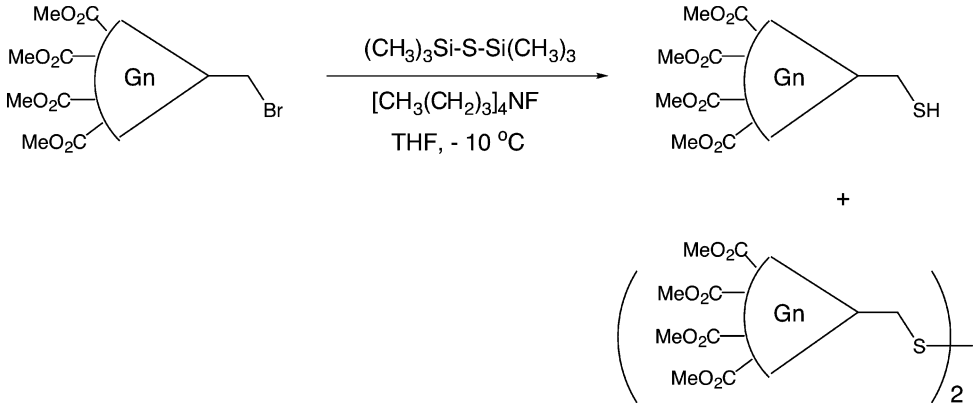

formation of unstable nanoparticles, especially in the reactions of (MeO_2C)G3-Br and (MeO_2C)G4-Br, suggested that the growing nanoparticle might have been noncovalently encapsulated by the dendrons. These experiments confirm our earlier suggestion[9] that formation of the NCDs may involve four steps, i.e., nucleation, growth, encapsulation, and passivation.

The ester-terminated NCDs were converted to the corresponding sodium carboxylates by treatment with sodium hydroxide, Scheme 2. In Au−G1(CO_2Me) and Au−G2(CO_2Me), complete hydrolysis of the ester groups occurred (as revealed by IR). In Au−G3(CO_2Me) and Au−G4(CO_2Me), residual ester peaks could be seen in the IR. Since the sodium salts obtained were soluble in water, further hydrolysis was not attempted. The sodium salts obtained (Au−G1(CO_2Na)−Au−G4(CO_2Na)) were black powders, soluble in water and insoluble in common organic solvents. Their solutions had colors resembling those of the esters.

Characterization of NCDs. The ester-terminated NCDs Au−G1(CO_2Me)−Au−G4(CO_2Me) and the sodium carboxylate terminated NCDs Au−G1(CO_2Na)−Au−G4(CO_2Na) were analyzed by several techniques, including HRTEM, TGA, and UV, IR, and NMR spectroscopies.

High-Resolution Transmission Electron Microscopy. HRTEM has provided extensive information about the size and, to a much lesser extent, the shapes of metal nanoparticles.[11] Figure 1 gives the HRTEM images of Au−G3(CO_2Me) and Au−G4(CO_2Me) (Figure 1 A, B) and the corresponding sodium carboxylates (Figure 1 C, D).

These images show that the NCDs are relatively small and do not possess a uniform core size. The core sizes exhibit a relatively wide distribution, as shown by the core-size histograms of the ester-terminated NCDs, given in Figure 2.

It can be seen from Figure 2 that the average core diameter increases as the NCD generation number increases. The linear average diameters of the populations of nanoparticles are given in Table 1. It is well-known that the core sizes of MPCs depend very much on reaction conditions. We have used only one set of reaction conditions, and it is quite conceivable that entirely different size distribution patterns might result if reaction conditions are varied. The distributions of core diameters of NCDs are comparable to those of MPCs prepared under similar conditions.

Thermogravimetric Analysis. For C_8-, C_{12}-, and C_{16}-coated MPCs, thermal decomposition occurred in a single, well-defined step of nearly 100 °C width, beginning at 230, 266, and 310 °C, respectively.[18] In contrast, for the NCDs reported earlier, the volatilization process occurred in two stages. The first stage, which contributed approximately 5% of the weight loss, was attributed to the removal of trapped solvent and TOAB,[9] followed by a second step in which dendritic fragments were lost. For the ester-terminated NCDs reported here, thermal decomposition occurred in three stages (see Supporting Information). The first stage, which contributed to ≤6% of the total weight loss, is attributed to the removal of TOAB and other trapped organics. The remaining two stages are attributed to the progressive removal of the dendrons. Details of the two-stage decomposition are not known at this time, but the percentage weights of dendrons in these NCDs calculated from the TGA results are presented in Table 1.

UV−Vis Spectroscopy. The absorption spectra of MPCs exhibit a smoothly increasing absorption at increasing energy (Mie scattering), with a superimposed surface plasmon band between 450 and 600 nm. The plasmon band responsible for the colors exhibited by the nanoparticles arises from interband transitions between the highly polarizable Au 5d[10] band and the unoccupied states of the conduction band. The intensity of the plasmon band is related to the particle size of the metal cluster. Hence, absorption spectroscopy is a very useful tool in the characterization of noble metal nanoparticles.[11,19] Absorption spectra of Au−G3(CO_2Me) and Au−G4(CO_2Me) and the corresponding sodium salts are shown in Figure 3.

Figure 3 shows that the absorption maximum and intensity of the plasmon bands increase from G1−G4 for the ester- and carboxylate-terminated NCDs. This result suggests increasing particle size in the order G1 < G2 < G3 < G4 and supports the results of the TEM studies. The plasmon band maxima for these NCDs are collected in Table 1.

FTIR Spectra. For alkanethiolate-protected MPCs, infrared spectroscopy provides valuable information regarding the conformation and ordering of the alkyl chains on the metal surface.[11,20] The frequency and bandwidth in the C−H and C−C stretching regions, in particular, are indicative of order in the MPC. In NCDs and arenethiolate MPCs, IR spectra were less

(18) Terrill, R. H.; Postlethwaite, T. A.; Chen, C.-H.; Poon, C.-D.; Terzis, A.; Chen, A.; Hutchison, J. E.; Clark, M. R.; Wignall, G.; London, J. D.; Superfine, R.; Falvo, M.; Johnson, C. S., Jr.; Samulski, E. T.; Murray, R. W. *J. Am. Chem. Soc.* **1995**, *117*, 12537.
(19) (a) Duff, D. G.; Baiker, A.; Edwards, P. P. *Langmuir* **1993**, *9*, 2301. (b) Wilcoxon, J. P.; Martino, A.; Baughmann, R. L.; Klavetter, E.; Sylwester, A. P. *Mater. Res. Soc. Symp. Proc.* **1993**, *286*, 131. (c) Kreibig, U.; Genzel, L. *Surf. Sci.* **1985**, *156*, 678.
(20) Hostetler, M. J.; Stokes, J. J.; Murray, R. W. *Langmuir* **1996**, *12*, 3604.

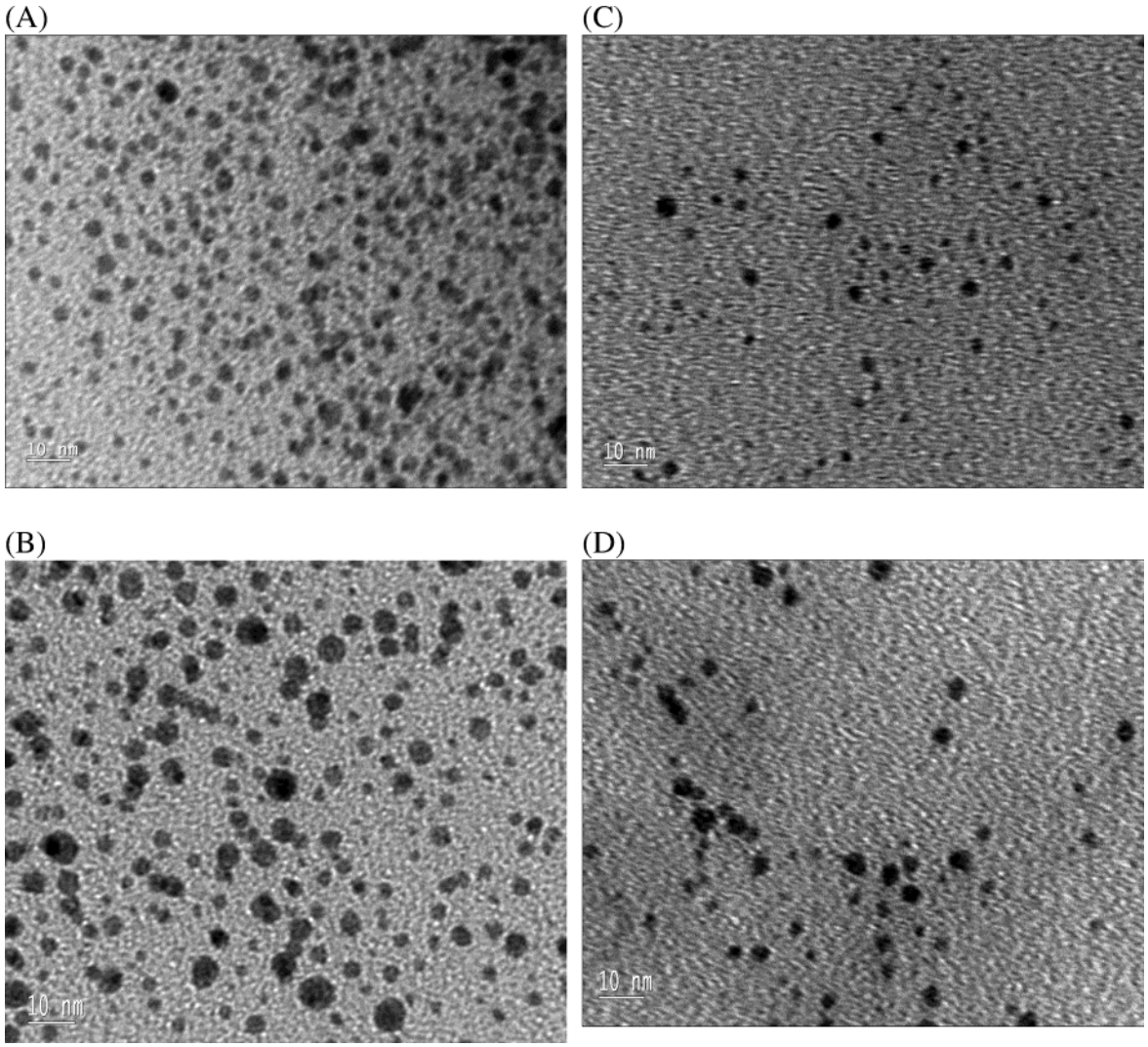

Figure 1. TEM images of (A) Au−G3(CO_2Me), (B) Au−G4(CO_2Me), (C) Au−G3(CO_2Na), and (D) Au−G4(CO_2Na).

useful. IR spectra of the ester-terminated disulfide dendrons and Au−G*n*(CO_2Me) were very similar, indicating that the vibrational modes in the dendrons are unaffected by their self-assembly on gold. Figure 4 presents the IR spectra of Au−G1(CO_2Me) and Au−G3(CO_2Me), showing identical absorption peaks.

Upon conversion to the corresponding sodium carboxylates, significant changes occurred in the IR spectra (Figure 4). The band at 1720 cm^{-1} for the ester carbonyl absorption disappeared, indicating that the hydrolysis is complete for Au−G1(CO_2Na), in which the strongest peak appeared at 1454 cm^{-1}. For Au−G3(CO_2Na), a small residual absorption is seen at 1720 cm^{-1}, indicating incomplete hydrolysis, with the strongest absorption at 1596 cm^{-1}. The IR spectra of the salts also show that the presence of adsorbed water, which could not be removed upon drying the samples under vacuum.

NMR Spectra. NMR spectra are not very useful in characterizing the NCDs. ^{1}H NMR and ^{13}C NMR of Au−G*n*(CO_2Me) (see Experimental Section) resembled those of the corresponding disulfide dendrons. In contrast to those of alkanethiolate protected MPCs,[11,21] ^{1}H signals of the methylene group directly attached to the sulfur atom did not exhibit any line broadening, but ^{1}H signals assigned to the outer phenyl groups had their bases slightly broadened, as observed for the NCDs reported earlier. ^{13}C NMR signals did not exhibit any broadening. Signals corresponding to TOAB could be seen in the ^{1}H and ^{13}C NMR of all Au−G*n*(CO_2Me). For the sodium salts, we could not obtain well-resolved ^{1}H NMR signals in D_2O.

Several reasons have been put forward to explain the NMR line broadening in MPCs but not in NCDs. Most important among these is the solidlike packing of the methylene chains closest to the Au core. Near the Au core, the methylene chains experience restricted motion, whereas those far removed from the core experience freedom of movement as in a liquid, leading to a broadening of NMR signals for groups near the core and relatively little or no broadening of signals for groups far removed from the core. In a typical NCD (Scheme 1), the CH_2−S groups attached to the metal core experience relatively little or no crowding, and steric congestion increases as one proceeds toward the exterior of the NCD. Thus, if NMR line broadening in NCDs were caused by steric crowding, broadening should be observed in the NMR signals of the outermost groups rather than at the core, in the reverse order of that seen in MPCs. Thus, local crowding probably explains the absence of NMR line broadening in NCDs.

(21) Badia, A.; Lennox, R. B.; Reven, L. *Acc. Chem. Res.* **2000**, *33*, 475.

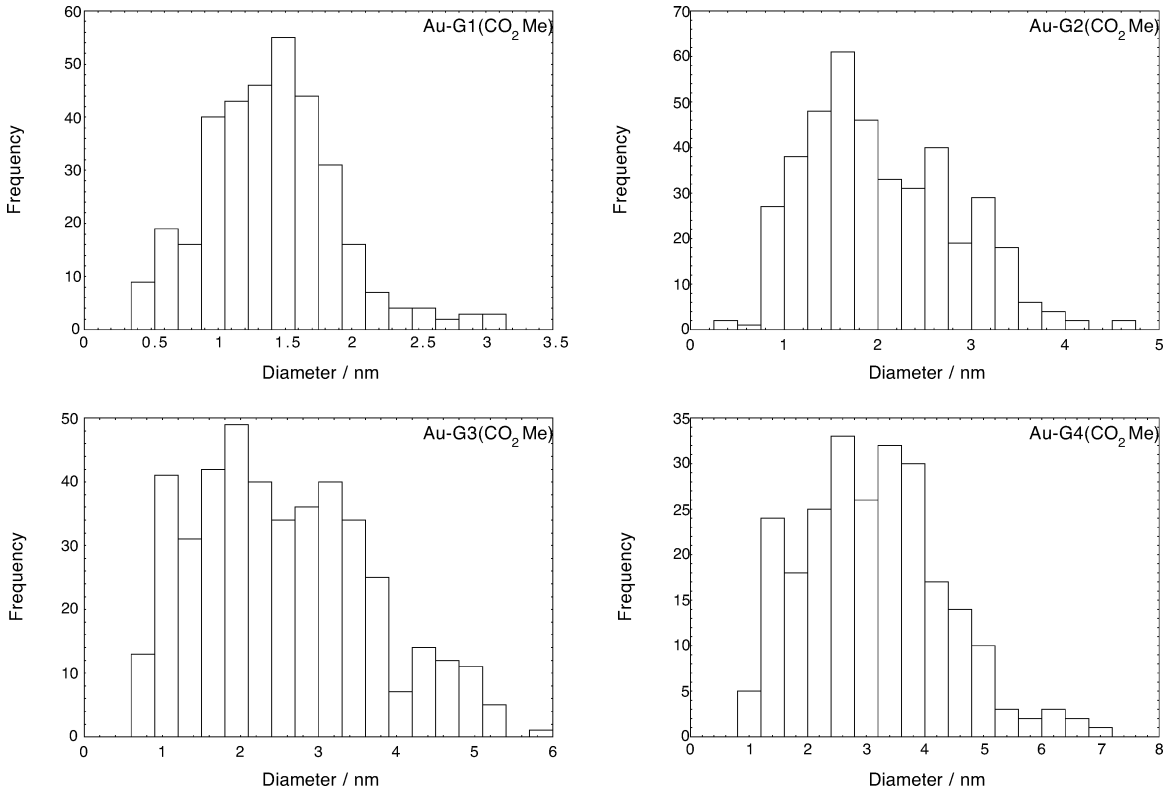

Figure 2. Core-size histograms for Au−G1(CO_2Me)−Au−G4(CO_2Me).

Table 1. TEM, TGA, and Absorption Spectral Data for Au−G*n*(CO_2Me)

Au-NCD	average core diameter (nm)	weight % Au	weight %[a] [(CO_2Me)Gn]-S	surface plasmon λ_{max} (nm)
Au−G1(CO_2Me)	1.40	74.46	23.54	485
Au−G2(CO_2Me)	2.04	63.86	35.14	510
Au−G3(CO_2Me)	2.54	62.26	32.74	522
Au−G4(CO_2Me)	3.10	60.05	33.95	524

[a] Corrected for adsorbed TOAB.

NaCN-Induced Decomposition of NCDs. Earlier work on alkanethiolate/gold self-assembled monolayers (SAM)[22] on planar gold surfaces and on alkanethiolate MPCs[1,11f] has shown that cyanide causes dissociation of the monolayer with concomitant etching or dissolution of the gold. In order for the cyanide to react with the gold, it must penetrate the protecting organic layer. The rate of decomposition of the SAM or MPC by NaCN can, therefore, be correlated to the extent of protection that the organic layer provides to the gold surface.

Our earlier experiments have shown that the gold cores of NCDs are also attacked by cyanide, and relative rates of cyanide-induced decomposition studies of Au−G*n*(CO_2Me) and Au−G*n*(CO_2Na) provide valuable insight into surface accessibility.

For Au−G*n*(CO_2Me), cyanide-induced decompositions were carried out in THF−H_2O (6:1) mixture. For the corresponding carboxylate salts, these reactions were carried out in aqueous solution. The relative rates of decomposition were obtained by monitoring absorption changes at 520 nm. In all cases, cyanide-induced decompositions were slower for the sodium salts than for the neutral ester. Figure 5 shows the changes in absorption as a function of time for G1 and G2 NCDs.

The decomposition reactions were very slow for G1 NCDs, but faster for other generations. In all cases, data were fit to a two-exponential function, $y = y_0 + a\exp(-k_1t) + b\exp(-k_2t)$.[11f] Fits of the data to this equation were very good for all Au-NCDs (correlation > 0.99), and the values of k_1 and k_2 obtained for the various NCDs are presented in Table 2.

The observation of two decomposition rate constants in these reactions is not well understood. We tentatively attribute this to the presence of two types of NCDs in each generation, one which has its surface relatively well covered by tightly packed dendrons and a second type which is relatively open. For the sodium carboxylates, the values of k_1 increased from G1 to G4. For the ester-terminated NCDs, k_1 for G2 was higher compared for G3 and G4. For G2−G4, values of k_2 were similar.

The shapes of Au−G*n*(CO_2Na)s are expected to be roughly spherical. In aqueous solutions, the salts will be fully ionized. These molecules thus have a layer of negative charge on the surface, and solution-phase anions are not expected to penetrate this Coulombic barrier and react with the gold, which is positioned at the center of the sphere. Cyanide ion penetrates this barrier because of its small size and because of imperfections on the NCD surface. The ionic barrier also explains why the reaction is slower for the sodium salts than for ester-terminated NCDs.

General Comments Regarding the Structure of NCDs. Results from the TEM and TGA studies provide useful information on the structure of the NCDs. From the TEM size distributions, one can obtain the average diameter of the nanoparticles (Table 1). This value can be used to approximate the number of gold atoms in the cluster using the density (59 atoms/nm^3) of bulk face-center cubic (fcc) Au. The approximate

(22) (a) Kumar, A.; Whitesides, G. M. *Appl. Phys. Lett.* **1993**, *63*, 2002. (b) Weisbecker, C. S.; Merritt, M. V.; Whitesides, G. M. *Langmuir*, **1996**, *12*, 3763. (c) Gorman, C. B.; Biebuyck, H. A.; Whitesides, G. M. *Chem. Mater.* **1995**, *7*, 252.

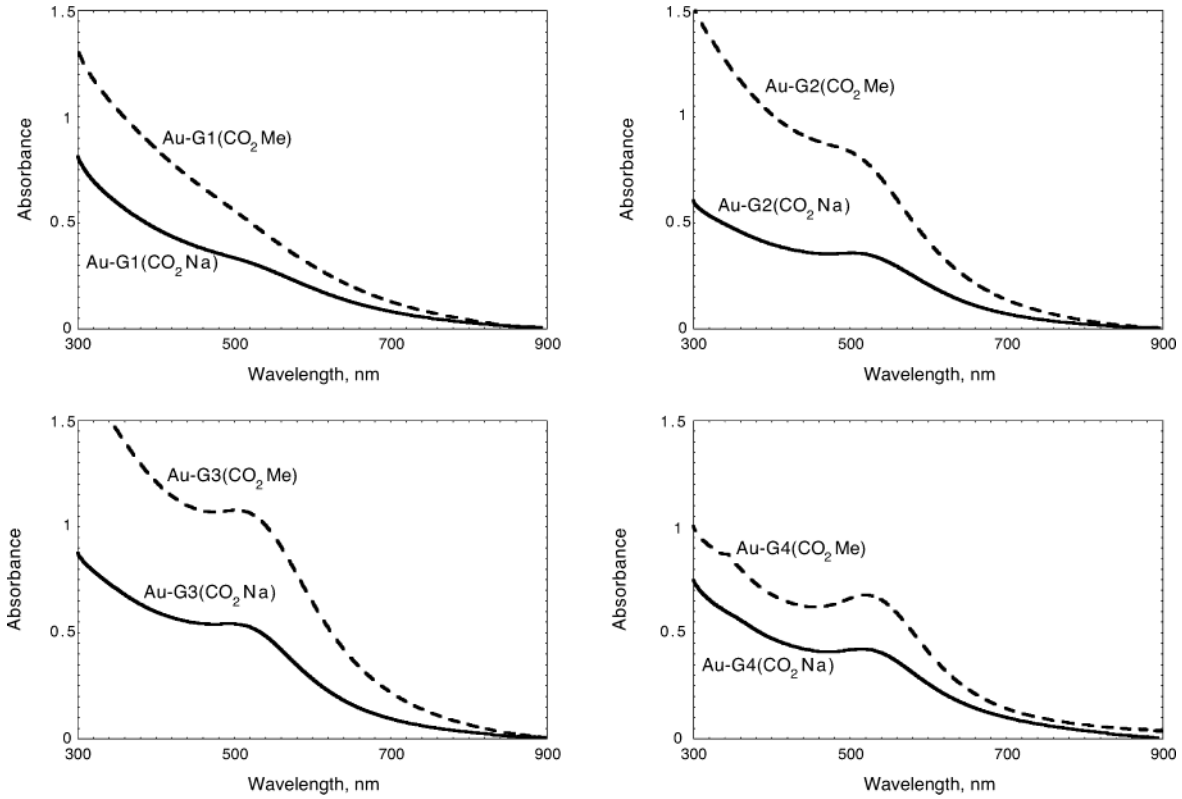

Figure 3. Absorption spectra of Au−G*n*(CO_2Me) in CH_2Cl_2 (dotted lines) and Au−G*n*(CO_2Na) in water (solid lines). Concentrations were ∼1 mg/10 mL.

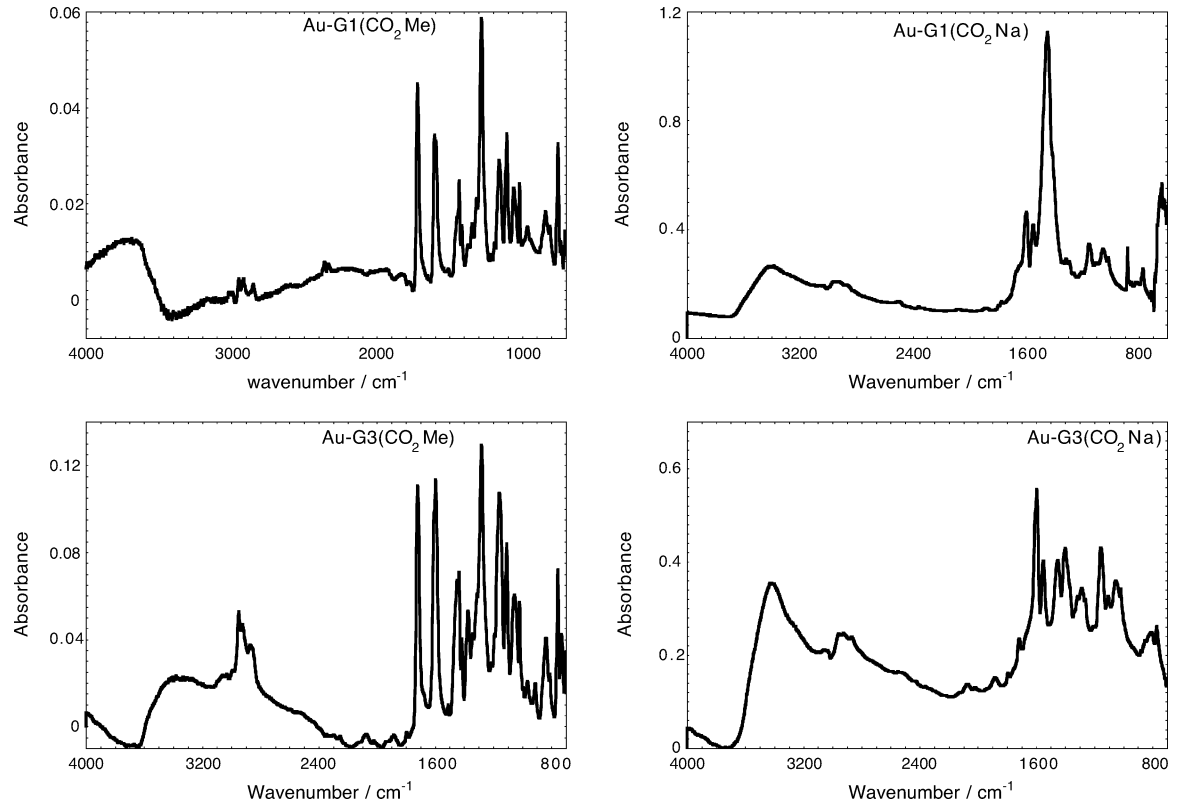

Figure 4. FT-IR absorbance spectra of Au−G1(CO_2Me), Au−G1(CO_2Na), AuG3(CO_2Me), and Au−G3(CO_2Na).

number of gold atoms in a cluster is given by the equation: $N_{Au} = (59\ nm^{-3})(\pi/6)(D)^3$, where D is the average diameter of the nanoparticle, in nanometers.[11s] The weight of the gold core is given by the equation $N_{Au} \times 197$ (197 = atomic weight of gold). This weight is equated to the weight percentage of gold from the TGA experiments to obtain the average total weight of the NCD. Given the percentage weight of the dendritic fraction (Table 1), we can calculate the total weight of the dendritic fraction in the NCD. This value, divided by the molecular weight of the dendritic thiol, gives the average number

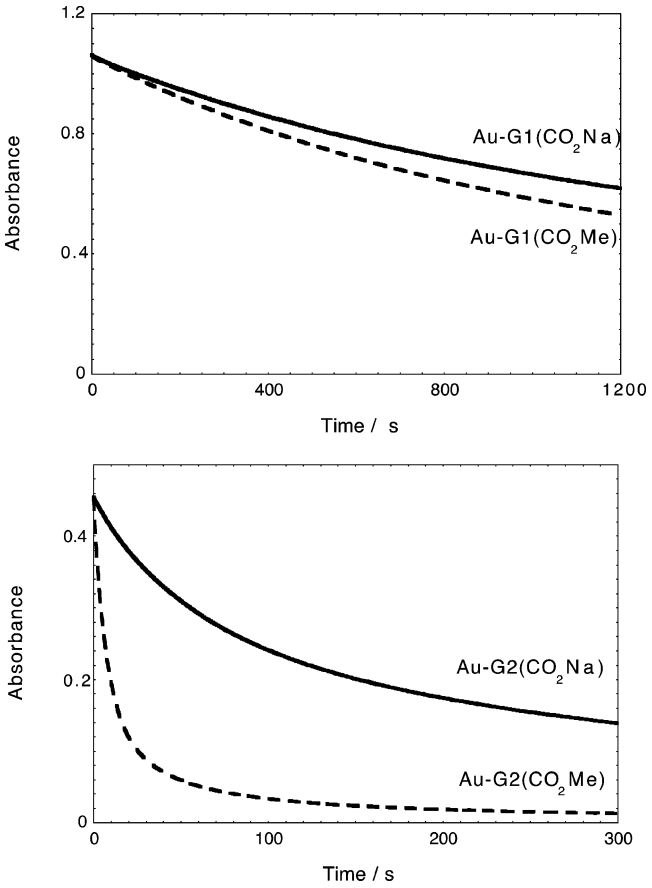

Figure 5. NaCN-induced decomposition of Au−G*n*. Absorbance changes were followed at 520 nm.

Table 2. Rate Constants for the Decomposition of Au-NCDs with NaCN

Au–NCD	k_1, s^{-1}	k_2, s^{-1}
Au−G1(CO_2Me)	$(1.04 \pm 0.03) \times 10^{-3}$	$(7.98 \pm 0.95) \times 10^{-4}$
Au−G2(CO_2Me)	$(1.26 \pm 0.04) \times 10^{-1}$	$(1.75 \pm 0.08) \times 10^{-2}$
Au−G3(CO_2Me)	$(9.16 \pm 0.04) \times 10^{-2}$	$(1.34 \pm 0.08) \times 10^{-3}$
Au−G4(CO_2Me)	$(1.15 \pm 0.02) \times 10^{-1}$	$(2.65 \pm 0.02) \times 10^{-2}$
Au−G1(CO_2Na)	$(9.28 \pm 0.29) \times 10^{-4}$	$(1.55 \pm 0.42) \times 10^{-4}$
Au−G2(CO_2Na)	$(1.67 \pm 0.04) \times 10^{-2}$	$(3.16 \pm 0.03) \times 10^{-3}$
Au−G3(CO_2Na)	$(1.75 \pm 0.06) \times 10^{-2}$	$(2.61 \pm 0.02) \times 10^{-3}$
Au−G4(CO_2Na)	$(2.08 \pm 0.09) \times 10^{-2}$	$(3.01 \pm 0.02) \times 10^{-3}$

of dendrimer units present on the nanoparticle core in each of the NCD generations.

In Table 3, we provide the calculated values of N_{Au}, the weight of the gold core, the weight of the dendritic fraction, and the average number of dendrons (rounded to the nearest integer) for all the NCD generations. The average number of dendrons attached to the unit surface area of the gold core was also calculated for each of the NCD generations. Since Au−G*n*(CO_2Na) were prepared from the esters by a hydrolysis reaction, we assume that values presented in the last two columns of Table 3 hold good for the corresponding generations of Au−G*n*(CO_2Na).

It can be seen from Table 3 that the number of dendrons/nm^2 follows the order G1 ≈ G2 > G3 > G4. For all cases of NCDs reported here, the occupancy/nm^2 is much lower than those reported for alkanethiolate (4.7/nm^2)- and arenethiolate (5−9/nm^2)-protected MPCs.[11l]

Our spectral measurements provide no direct evidence for the presence of gold−sulfur bonds in the NCDs, and one might argue that the gold clusters may be present as trapped materials rather than structural units of the dendrimer. This possibility is ruled out for several reasons. First, the reaction mixture contains only dendrons and not dendrimers. Dendrons, particularly the lower-generation ones, typically do not possess encapsulation properties. Furthermore, the surface areas of the gold cores are larger than those of the dendrons, and thus encapsulation is not physically possible. Examples of nanoparticles encapsulated in PAMAM dendrimers (G ≥ 4) are available in the literature.[7] The diameter of the 4G PAMAM dendrimer is 4 nm, which is much larger than the metallic nanoparticle or the Fréchet-type dendrons used in this study.

A model wherein several dendrons assemble a cavity for encapsulation of the nanoparticle can also be considered. This model, however, is not supported by the control experiments with dendritic bromides. Control experiments with (MeO_2C)-G3-Br and (MeO_2C)G4-Br showed that gold nanoparticles could be stabilized to some extent by TOAB and dendrons. In these cases, the particles aggregate and precipitate when TOAB is removed. In contrast, solutions of nanoparticles obtained in the presence of the disulfides were stable for over two months and no precipitation was noted in any of these solutions. Aqueous solutions of Au−G*n*(CO_2Na) similarly showed no evidence of precipitation, indicating no protection by encapsulation. Nor do decomposition studies with cyanide ion support the encapsulation model. If the gold particles were protected by encapsulation, then protection should be greater for larger dendrons, which is not observed experimentally.

Micellar Properties of Au−G*n*(CO_2Na). Micellar properties of dendritic molecules are usually probed by spectral shifts of dye molecules or by studies of the solubilization of hydrocarbons or fatty alcohols.[16] For example, pinacyanol chloride (PC) is traditionally used as a spectrophotometric probe to study micellar properties.[16q] In aqueous solution, PC shows absorption bands at 549 and 601 nm. These absorption bands shift to 564 and 610 nm, respectively, in SDS micelles. Similar spectral shifts were observed for PC in the presence of dendritic unimolecular micelles.[16q] Figure 6 shows the absorption spectra of PC (1×10^{-5} M) in water (pH =7) and aqueous Au−G*n*(CO_2Na) solutions.

Thus, the absorption bands of PC are red-shifted (∼20 nm) in the presence of Au−G*n*(CO_2Na), as would be expected if aqueous solutions of Au−G*n*(CO_2Na) possessed micellar properties, Figure 6.

Figure 6 also presents a comparison of the influence of the size (generation) of the Au−G*n*(CO_2Na) on the observed spectral shift. In all cases presented in Figure 6 (PC, A−D), PC is present at the same concentration, but the absorption intensity is different in the presence of the different NCD generations. Without a partner complexant, PC adheres to the glass surface and forms aggregates: an aqueous solution of PC loses about 40% of its absorption intensity at 549 and 601 nm, if the sample is kept at room temperature for 1 day. The spectrum labeled "PC" in Figure 6 was taken immediately after preparation of the solution. The other samples were allowed to equilibrate for 1 day. During this time, the nonmicellized fraction either aggregated or adhered to the glass surface. Figure 6 shows that a solution of Au−G4(CO_2Na) micellizes PC completely, producing a stable solution from which further aggregation is

Table 3. Calculated NCD Parameters

Au–NCD	no. of core Au atoms	wt. of Au core	wt. of dendritic fraction	mol. wt. of Ar–S unit	no. of wedges/particle	no. of dendrons/nm^2
Au−G1(CO_2Me)	85	16,745	5,293.8	451	11.7	1.90
Au−G2(CO_2Me)	262	51,614	28,410.3	991	28.7	2.19
Au−G3(CO_2Me)	506	99,682	52,418.7	2071	25.3	1.25
Au−G4(CO_2Me)	920	181,240	102,466.2	4231	24.2	0.80

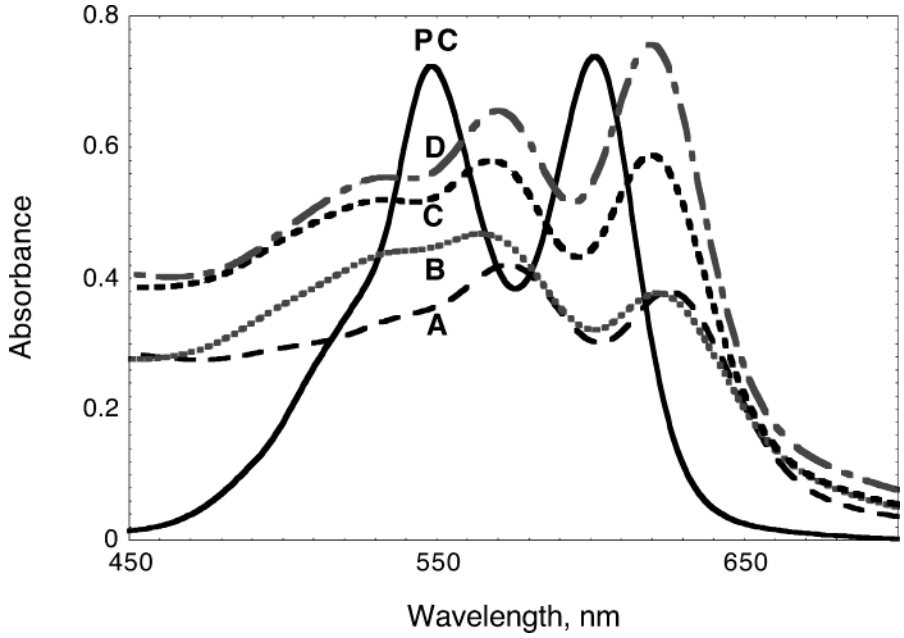

Figure 6. Absorption spectra of pinacyanol chloride (1×10^{-5} M) in water (PC) and in aqueous solutions of (A) Au−G1(CO_2Na), (B) Au−G2(CO_2Na), (C) Au−G3(CO_2Na), and (D) Au−G4(CO_2Na). [Au−G*n*(CO_2Na)] were ∼1 mg/10 mL water.

suppressed. For lower-generation NCD salts, micellization of PC is less complete, resulting in lower absorption intensities.

It has been widely documented[14] that the solubility of hydrophobic compounds in water can be dramatically enhanced by the addition of surfactant molecules above their cmc. If Au−G*n*(CO_2Na)s have micellar properties, then it would be expected that the solubility of hydrophobic molecules in water would increase in the presence of Au−G*n*(CO_2Na). We have studied the solubilization of pyrene in aqueous solutions of Au−G*n*(CO_2Na) (see Experimental Section for details). The solubility of pyrene in aqueous Au−G*n*(CO_2Na) solutions is plotted against the generation number of the solubilizing NCD in Figure 7. The solubility of pyrene in water is 8×10^{-7} M. Figure 7 shows that the solubility of pyrene was increased to $\sim 3 \times 10^{-4}$ M (∼300-fold) by the addition of Au−G*n*(CO_2Na). As in the case of PC, we anticipated that solubility of pyrene would increase with the NCD generation number. This trend, if observed at all, is very weak.

Au-NCDs as Nanoreactors. Metal nanoparticle-cored dendrimers have several interesting structural features which make them ideal candidates as "nanoreactors." These materials have a metal core of 1.5−4.0 nm diameter. The present study deals with only gold nanoparticles, but the same concepts can be extended easily to several other catalytically active transition metals.[23] Since heterogeneous catalysis takes place on the surface of the metal, many catalysis methods seek to maximize available surface area by reducing the size of the catalytic particle. Unprotected nanometer-sized metal particles, however, have a tendency to aggregate, which leads to a reduction of the observed catalytic activity. Metal nanocatalysts are usually prepared by evaporation/condensation of the metal or by chemical/electrochemical reduction of metal salts. To control the particle size and prevent agglomeration, stabilizers such as polymers, ligands, or surfactants are generally used in these reactions. This process leads to partial passivation of the catalyst surface and thus reduces the catalytic activity. Thus, there is a need for new nanoparticle technologies that provide the highest protection and least passivation of the nanoparticle surface.

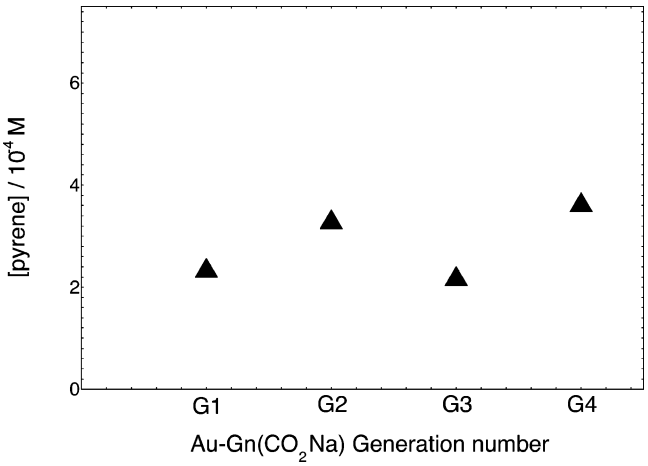

Figure 7. Solubility of pyrene in aqueous Au−G*n*(CO_2Na) solutions.

(23) (a) Schmidt, G., Ed.*Clusters and Colloids*; VCH: Weinheim, 1994. (b) Hayat, M. A., Ed. *Colloidal Gold: Principles, Methods and Applications*; Academic: San Diego, 1991. (c) Feldheim, D. L.; Foss, C. A., Jr., Eds. *Metal Nanoparticles: Synthesis, Characterization and Applications*; Marcell Dekker: New York, 2002.

Scheme 4. Structural Features of Au−G*n*(CO_2Na) Salt NCDs

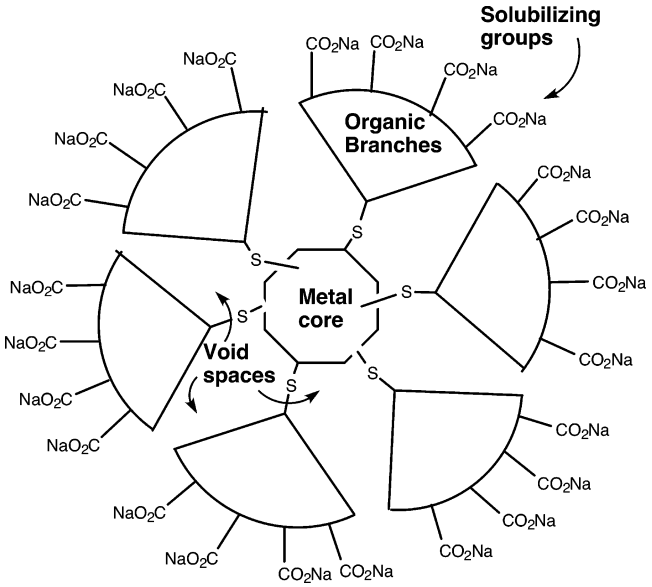

The NCDs present an excellent solution to this problem. The NCDs described here (and also in our earlier report[9]) are very stable and have diameters in the 1.5−4.0 nm range. Table 3 shows that Au−G4(CO_2Me), having a diameter of 3.1 nm, has only 24 dendritic units attached to the gold core. Alkanethiolate MPCs with similar core diameters have ∼350 alkyl chains attached to the core.[11k] Thus, compared to alkanethiolate MPCs, Au−G4(CO_2Me) has only 8% of its surface atoms passivated by covalent bond formation. The remaining 92% of the surface atoms are free to participate in catalytic reactions, provided the target molecules can penetrate the porous dendritic framework to access the catalyst surface.

Some interesting structural features of Au−G*n*(CO_2Na) are presented in Scheme 4. As mentioned above, the surface of the metal core is largely unpassivated. Au−G*n*(CO_2Na) salts have a negatively charged outer surface, which enables them to dissolve in aqueous solutions and to exhibit micellar properties. They also possess a relatively nonpolar organic branching region, which could provide cavities for guest molecules. The size and structure of the cavities will depend on the chemical constitution of the dendrons. The driving force for guest transportation into and out of these cavities is affected by electrostatic interactions, complexation reactions, steric confinement, various types of weak nonbonded forces (van der Waals, hydrogen bonding, hydrophobic forces, etc.), or combinations thereof. Thus, by varying the structure of the dendrons, different types of guests can be encapsulated within the dendrons, to a position from which the substrate can access the core metal catalyst.

Another very important structural feature of NCDs is the large void spaces present close to the metal surface. Since there are only a few dendritic units on the surface, these cavities should be relatively large. These voids can act as guest cavities, and because they are on the metal surface, they can also function as "reaction vessels" for catalytic reactions. Thus, the NCD can bring reactants into its interior, where catalytic reactions (e.g., hydrogenation) can take place. All these features make the NCDs ideally suited as nanoreactors for metal-catalyzed reactions.

We have recently synthesized and characterized a palladium nanoparticle-cored G3 dendrimer (Pd−G-3).[24] Preliminary investigations have shown that Pd−G-3 can act as catalyst in important C−C bond-forming reactions such as the Heck and Suzuki reactions. Micelle-forming NCDs will advance this concept further by catalyzing these reactions in water. Using water as solvent for organic reactions has obvious advantages of cost, safety, and environmental concerns.[25] Thus, catalytically active NCD micelles will have very important potential applications.

Conclusions

The syntheses and characterization of gold nanoparticle-cored dendrimers with ester terminal groups and their hydrolyzed variants are reported. TEM, TGA, UV, IR, and NMR spectroscopies show the density of the branching units connected to the core to decrease from 1.90/nm^2 for Au−G1(CO_2Me) to 0.80/nm^2 for Au−G4(CO_2Me). When the ester-terminated NCDs are hydrolyzed with NaOH, the resulting sodium salts were water soluble and exhibited micellar properties, as evidenced by spectral shifts of included dye molecules. Because of the dendritic structure, Au−G*n*(CO_2Me) and Au−G*n*(CO_2-Na) enclose large void spaces near the metal cluster that can act as host cavities for guest molecules. Because a large fraction of the surface area of the metallic core of the NCD is unpassivated, the core metal cluster should exhibit good catalytic activity. Thus, NCDs can act as micellar hosts as well as potential catalysts. These properties make them ideal candidates as catalytic nanoreactors.

Experimental Section

Chemicals. 3,5-Dihydroxybenzoic acid, methyl 4-bromomethylbenzoate, carbon tetrabromide, triphenylphosphine, 18-crown-6 ether, $HAuCl_4$, tetraoctylammonium bromide (TOAB), $NaBH_4$, pinacyanol chloride, and pyrene were used as received. Solvents such as toluene, acetone, absolute ethanol, and dichloromethane were used as received. THF was freshly distilled from sodium benzophenone ketyl. Spectroscopic grade solvents were used for spectral measurements. Water was obtained from a Millipore Nanopure water system.

Synthesis of (CO_2Me)G1-SH and (CO_2Me)G1-S−S-G1(CO_2Me). These were prepared from ($MeCO_2$)G1-Br. A stirred solution of ($MeCO_2$)G1-Br (4 mM) in freshly distilled THF (25 mL) was cooled to −10 °C, and hexamethyldisilathiane (5 mM) and Bu_4NF (4.8 mM) were added. The resulting mixture was then stirred at room temperature overnight. The mixture was diluted with CH_2Cl_2 (50 mL) and washed with saturated NH_4Cl solution. CH_2Cl_2 was removed, and the residue was chromatographed over silica gel. Elution with CH_2Cl_2 gave the thiol, **(CO_2Me)G1-SH**: yield 40%, mp 123−124 °C; IR 2950, 2571, 1725, 1609, 1596, 1442, 1284, 1175, 1109, 1070, 1019 cm^{-1}; ^{1}H NMR ($CDCl_3$) δ 1.76 (t, 1 H, J = 8 Hz, S*H*), 3.67 (d, 2 H, J = 8 Hz, CH_2S), 3.92 (s, 6 H, OCH_3), 5.09 (s, 4 H, ArCH_2O), 6.46 (t, 1 H, J = 2 Hz, Ar*H*), 6.58 (d, 2 H, J = 2 Hz, Ar*H*), 7. 48 and 8.05 (ABq, 8 H, J = 8 Hz, Ph*H*); ^{13}C NMR ($CDCl_3$) δ 29.39 (*C*H$_2$SH), 52.40 (O*C*H$_3$), 69. 60 (Ar*C*H$_2$O), 100.97, 107.72, 127.22, 129.95, 130.12, 142.16, 143.90, 160.03 (Ar*C*), 167.01 (*C*═O). FAB Mass; Calcd 452.1294; Found 452.12943.

Further elution with CH_2Cl_2 gave the disulfide, **(CO_2Me)G1-S−S-G1(CO_2Me)**: yield 49%, mp 143−144 °C; IR 2951, 1722, 1595, 1436, 1280, 1164, 1108, 1066, 1020 cm^{-1}; ^{1}H NMR ($CDCl_3$) δ 3.51 (s, 2 H,

(24) Gopidas, K. R.; Whitesell, J. K.; Fox, M. A. *Nano Lett.* **2003**. Manuscript submitted for publication.
(25) (a) Lindström, U. M. *Chem. Rev.* **2002**, *102*, 2751. (b) Greico, P. A., Ed. *Organic Synthesis in Water*; Blackie Academic & Professional: London, 1998.

CH_2S), 3.91 (s, 6 H, OCH_3), 5.06 (s, 4 H, ArCH_2O), 6.47−6.53 (m, 3 H, Ar*H*), 7.44 and 8.01 (ABq, 8 H, J = 8 Hz, Ph*H*); ^{13}C NMR δ 36.02 (*C*H_2S), 52.39 (O*C*H_3), 69.56 (Ar*C*H_2O), 101.02, 108.52, 127.22, 129.93, 130.09, 140.89, 142.10, 159.87 (Ar*C*), 166.99 (*C*═O).

Synthesis of (CO$_2$Me)G2-SH and (CO$_2$Me)G2-S−S-G2(CO$_2$Me). This was prepared from (MeCO$_2$)G2-Br by a similar procedure. Elution of the column with a mixture of CH_2Cl_2 and ether (9:1) gave the thiol, **(CO$_2$Me)G2-SH**: yield 10%, becomes glasslike above 120 °C; IR 2949, 1719, 1596, 1436, 1280, 1163, 1107, 1060, 1018; ^{1}H NMR δ 1.76 (t, 1 H, J = 7 Hz, S*H*), 3.66 (d, 2 H, J = 7 Hz, ArCH_2S), 3.92 (s, 12 H, OCH_3), 4.96 and 5.09 (each s, 12 H, ArCH_2O), 6.42−6.66 (m, 9 H, Ar*H*), 7.47 and 8.04 (ABq, 16 H, J = 8 Hz, Ph*H*); ^{13}C NMR δ 29.41 (*C*H_2S), 52.39 (O*C*H_3), 69.47, 70.04 (Ar*C*H_2O), 100.92, 101.86, 106.71, 107.49, 127.21, 129.96, 130.12, 139.69, 142.12, 143.67, 160.09 (Ar*C*), 167.00 (*C*═O). FAB Mass; Cald 992.3078; Found: 992.30750.

Further elution with CH_2Cl_2−ether mixture (4:1) gave the disulfide, **(CO$_2$Me)G2-S−S-G2(CO$_2$Me)**, colorless glass: yield 80%; IR 2996, 2940, 1726, 1596, 1435, 1373, 1274, 1155, 1109, 1055, 1019 cm^{-1}; ^{1}H NMR ($CDCl_3$) δ 3.51 (s, 2 H, C*H*$_2$S), 3.89 (s, 12 H, OCH_3), 4.89−5.01 (m, 12 H, ArCH_2O), 6.45−6.63 (m, 9 H, Ar*H*), 7.40 and 7.99 (ABq, 16 H, J = 8 Hz, Ph*H*); ^{13}C NMR ($CDCl_3$) δ 36.23 (*C*H_2S), 52.37 (O*C*H_3), 69.54, 69.99 (Ar*C*H_2O), 101.72, 101.77, 106.67, 106.71, 108.35, 108.75, 127.17, 129.90, 130.07,139.62, 139.67, 139.97, 140.84, 142.09, 159.92, 159.96, 160.06 (Ar*C*), 166.97 (*C*═O).

Synthesis of (CO$_2$Me)G3-S−S-G3(CO$_2$Me). This was prepared from (MeCO$_2$)G3-Br (0.5 mM) using hexamethyldisilathiane (1.25 mM) and Bu$_4$NF (1.2 mM). The product was worked up by column chromatography (elution with CH_2Cl_2−ether (9:1)). The product was purified several times by dissolving in CH_2Cl_2 and precipitating into ether, and then drying under vacuum for 24 h: colorless glass, yield 82%; IR 2950, 1718, 1596, 1436, 1415, 1279, 1158, 1108, 1053, 1019, 837, 755 cm^{-1}; ^{1}H NMR ($CDCl_3$) δ 3.50 (s, 2 H, C*H*$_2$S), 3.87 (s, 24 H, OCH_3), 4.76−4.95 (m, 28 H, ArCH_2O), 6.41−6.59 (m, 21 H, Ar*H*), 7.38 and 7.97 (ABq, 32 H, J = 8 Hz, Ph*H*); ^{13}C NMR ($CDCl_3$) δ 36.04 (*C*H_2S), 52.12 (O*C*H_3), 69.24, 69.68 (Ar*C*H_2O), 101.386, 101.48, 106.31, 106.44, 126.93, 127.17, 129.63, 129.80, 139.26, 139.35, 140.75, 141.82, 159.67, 159.78, 159.89 (Ar*C*), 166.71 (C═O).

Synthesis of (CO$_2$Me)G4-S−S-G4(CO$_2$Me). This was prepared from (MeCO$_2$)G4-Br (0.1 mM) using hexamethyldisilathiane (1.25 mM) and Bu$_4$NF (1.2 mM). The product was worked up by column chromatography (elution with CH_2Cl_2−ether (9:1)). The product was purified several times by dissolving in CH_2Cl_2 and precipitating into ether and then drying under vacuum for 24 h: colorless glass, yield 35%; IR 2950, 1720, 1596, 1447, 1415, 1279, 1157, 1109, 1056, 1020, 837, 755 cm^{-1}; ^{1}H NMR ($CDCl_3$) δ 3.51 (s, 2 H, C*H*$_2$S), 3.87 (s, 48 H, OCH_3), 4.88−5.03 (m, 60 H, ArCH_2O), 6.47−6.70 (m, 45 H, Ar*H*), 7.40 and 7.99 (ABq, 64 H, J = 8 Hz, Ph*H*); ^{13}C NMR ($CDCl_3$) δ 29.71 (*C*H_2S), 52.12 (O*C*H_3), 69.31, 69.53, 69.76, 69.90 (Ar*C*H_2O), 101.53, 106.32, 106.42,126.48, 126.94, 127.18, 129.65, 129.83, 130.03, 139.29, 139.39, 141.85, 159.81, 159.94, 160.00 (Ar*C*), 166.71 (C═O).

General Procedure for Synthesis of NCDs. To a stirred solution of tetraoctylammonium bromide (0.342 g, 6.24 × 10^{-4} M) in toluene (20 mL) was added a solution of hydrogen tetrachloroaurate (0.085 g, 2.5 × 10^{-4} M) at room temperature. After stirring for 10 min the orange toluene layer was separated. To this solution was added a solution of the disulfide (0.2 g for Au−G1(CO$_2$Me) and Au−G2(CO$_2$Me), 0.1 g for Au−G3(CO$_2$Me) and Au−G4(CO$_2$Me)) in CH_2Cl_2 (5 mL). The mixture was stirred and cooled in ice (0−2 °C), and a solution of sodium borohydride (0.1 g, 2.5 × 10^{-3} M) in water (6 mL) was added. After 30 min the ice bath was removed, and stirring was continued for 2 d. The black toluene layer was separated, and the toluene was removed by rotary evaporation at 50 °C. The black residue obtained was sonicated with ethanol (20 mL) for 5 min and allowed to settle. The supernatant liquid was decanted. This procedure was repeated (∼20 times) until the supernatant ethanol became clear and colorless immediately after sonication. The ethanol was then decanted, and the sample first dried in air and then under vacuum for 2 days. Yield of NCDs varied between 20 and 30 mg. IR and NMR data for the NCDs are given below.

Au−G1(CO$_2$Me): IR 2917, 1721, 1604, 1435, 1415, 1281, 1161, 1108, 1060, 1020, 841, 755 cm^{-1}; ^{1}H NMR ($CDCl_3$) δ 3.51(s, 2 H, C*H*$_2$S), 3.91 (s, 6 H, OCH_3), 5.04 (s, 4 H, ArCH_2O), 6.47−6.53 (m, 3 H, Ar*H*), 7.45 and 8.01 (ABq, 8 H, J = 8 Hz, Ph*H*); ^{13}C NMR ($CDCl_3$) δ 36.02 (*C*H_2S), 52.39 (O*C*H_3), 69.58 (Ar*C*H_2O), 101.03, 108.51, 108.89, 127.22, 129.76, 129.94, 130.10, 140.88, 142.09, 159.86 (Ar*C*), 167.00 (C═O). Peaks corresponding to TOAB were present in the ^{1}H and ^{13}C NMR.

Au−G2(CO$_2$Me): IR 2952, 1721, 1597, 1436, 1416, 1281, 1159, 1109, 1055, 1020, 841, 756 cm^{-1}; ^{1}H NMR ($CDCl_3$) δ 3.52 (s, 2 H, C*H*$_2$S), 3.90 (s, 12 H, OCH_3), 4.90−5.02 (m, 12 H, Ar CH_2O), 6.48−6.63, (m, 9 H, Ar*H*), 7.42 and 8.00 (ABq, 16 H, J = 8 Hz, Ph*H*); ^{13}C NMR ($CDCl_3$) δ 36.00 (*C*H_2S), 52.14 (O*C*H_3), 69.33, 69.78 (Ar*C*H_2O), 100.97, 101.56, 106.49, 108.13, 126.95, 129.57, 129.70, 129.85, 139.20, 139.45, 140.61, 141.86, 159.74, 159.84, 159.97 (Ar*C*), 166.77 (C═O). Peaks corresponding to TOAB were present in the ^{1}H and ^{13}C NMR.

Au−G3(CO$_2$Me): IR 2950, 1720, 1597, 1436, 1416, 1280, 1158, 1109, 1055, 1020, 839, 756 cm^{-1}; ^{1}H NMR ($CDCl_3$) δ 3.50 (s, 2 H, C*H*$_2$S), 3.87 (s, 24 H, OCH_3), 4.79−5.06 (m, 28 H, ArCH_2O), 6.41−6.49 (m, 21 H, Ar*H*), 7.38 and 7.97 (ABq, 32 H, J = 8 Hz, Ph*H*) (the integrations were not very good); ^{13}C NMR ($CDCl_3$) δ 36.00 (*C*H_2S), 52.13 (O*C*H_3), 69.24, 69.38, 69.68 (*C*H_2O), 100.97, 101.37, 101.48, 106.30, 106.44, 108.02, 126.93, 129.63, 129.80, 139.24, 139.34, 140.74, 141.81, 159.661, 159.77, 159.89 (Ar*C*), 166.71 (C═O). Peaks corresponding to TOAB were present in the ^{1}H and ^{13}C NMR.

Au−G4(CO$_2$Me): IR 2950, 1721, 1597, 1448, 1416, 1374, 1281, 1159, 1109, 1055, 1020, 838, 756 cm^{-1}; ^{1}H NMR ($CDCl_3$) δ 3.45, (s, C*H*$_2$S), 3.83 (s, OCH_3), 4.70−5.01 (m, Ar CH_2O), 6.41−6.63, (m, Ar*H*), 7.33 and 7.93 (ABq, J = 8 Hz, Ph*H*) (integrations were not very good); ^{13}C NMR ($CDCl_3$) δ 52.09 (O*C*H_3), 69.17, 69.32, 69.64 (*C*H_2O), 101.40, 101.53, 106.41, 126.89, 126.96, 129.56, 129.66, 129.75, 129.83, 139.46, 141.79, 159.74, 159.82 (Ar*C*), 166.66 (C═O). The *C*H_2S peak was not observed. Peaks corresponding to TOAB were present in the ^{1}H and ^{13}C NMR.

General Procedure for the Hydrolysis of Au−G*n*(CO$_2$Me). Au−G-*n*-(CO$_2$Me) (30 mg) was suspended in a mixture of absolute ethanol (36 mL) and aqueous NaOH (20%, 4 mL). The mixture was stirred for 2 d before being filtered and washed with 90% ethanol and then with absolute ethanol. The sample was then dried in a vacuum for 4 d. IR data for Au−G*n*(CO$_2$Na) are given below.

Au−G1(CO$_2$Na): IR 1596, 1549, 1449, 1154, 1055, 880, 771 cm^{-1}.

Au−G2CO$_2$Na): 1596, 1551, 1454, 1156, 1053, 866, 771, 679 cm^{-1}.

Au−G3(CO$_2$Na): 2925, 1596, 1552, 1451, 1401, 1286, 1155, 1053, 807, 771 cm^{-1}.

Au−G4(CO$_2$Na): 2949, 1718 (unhydrolyzed ester), 1596, 1553, 1449, 1400, 1281, 1156, 1108, 1052, 1018, 834, 770 cm^{-1}.

Spectroscopy. Infrared absorbance spectra were acquired using a Nicolet 510P FT-IR spectrometer. For the dendrons wedges and Au−G*n*(CO$_2$Me), IR spectra were recorded using dropcast thin films on KBr plates. For Au−G*n*(CO$_2$Na) powdered samples were pressed into a pellet with KBr. UV−vis spectra were collected using a Shimadzu UV-3101PC UV−vis−NIR scanning spectrophotometer. The ^{1}H and ^{13}C NMR spectra of $CDCl_3$ solutions were collected at 400 and 100 MHz, respectively, on a Varian Mercury 400 spectrometer. The FAB mass spectrum was obtained with a JEOL HX110HF mass spectrometer. The TGA experiments were performed on a TA Instruments Hi-Res TGA 2950 thermogravimetic analyzer. High-resolution transmission electron microscopy images of the particles were obtained with a side-entry Phillips CM12 electron microscope operating at 120 keV. Samples of Au−G*n*(CO$_2$Me) for TEM were prepared by drop-casting one drop of a ∼1 mg/mL NCD solution in CH_2Cl_2 onto standard carbon-coated Formvar films on copper grids (300 mesh) and drying in air for 30 min. For the TEM of Au−G*n*(CO$_2$Na), samples were prepared from

aqueous solutions. For each sample, two typical regions were scanned. The average cluster diameters were obtained using Scion Image software.

Decomposition by Cyanide. The NaCN induced decomposition studies of Au−G*n* were performed as follows: THF solutions of Au−G*n*(CO_2Me), having an optical density in the range of 1−2, were prepared. Three-milliliter samples of these solutions were quickly mixed with 0.5 mL of aqueous solutions (10.5 mmol) of NaCN (final [NaCN] = 1.5 mM). The changes in absorbance at 520 nm were monitored for 1200 s for Au−G1 and for 300 s for other NCD generations. For the decomposition studies of Au−G*n*(CO_2Na), 3 mL of aqueous solutions were mixed with 0.5 mL of NaCN solution. The solutions obtained at the end of the decomposition experiments were nearly colorless.

Micellization Experiments. Micellization experiments with pinacyanol chloride were carried out as follows. Aqueous solutions of Au−G*n*(CO_2Na) (∼1 mg/10 mL) containing PC (1×10^{-5} M) were sonicated for 15 min and then allowed to equilibrate in the dark for 1 d, before recording the UV spectra.

For pyrene solubilization experiments, the following procedure was adopted. Powered pyrene samples (10 mg each) were added to aqueous Au−G*n*(CO_2Na) solutions (10 mL, each containing 2 mg of Au−G*n*(CO_2Na)). The samples were sonicated for 2 h and then allowed to equilibrate for 2 d. The solutions were filtered and washed with water (50 mL), and the pyrene was extracted into CH_2Cl_2 (3×25 mL). The dichloromethane extracts were combined and concentrated to 10 mL, and the concentration of pyrene was determined by UV. The extinction coefficient of pyrene absorption at 337 nm is taken as 4.9×10^4 M^{-1} cm^{-1} for the calculation of pyrene concentration.

Acknowledgment. This work was supported by the Chemistry Division, Office of Basic Energy Sciences, U.S. Department of Energy under Grant Number DE-FG02-01ER15280. K.R.G. thanks the Regional Research Laboratory (CSIR), Trivandrum for a one-year sabbatical leave to NCSU.

Supporting Information Available: Thermograms of Au−G1(CO_2Me)−AuG4-(CO_2Me). This material is available free of charge via the Internet at http://pubs.acs.org.

JA036626H